Chemical Substituent Effects on Morphological Transitions in Styrene−Butadiene−Styrene Triblock Copolymer Grafted with Polyhedral Oligomeric Silsesquioxanes

Daniel B. Drazkowski,[†] Andre Lee,*[,†] Timothy S. Haddad,[‡] and David J. Cookson[§]

Department of Chemical Engineering & Materials Science, Michigan State University, East Lansing, Michigan 48823; ERC, Inc., Air Force Research Laboratory, PRSM, Bldg. 8451, 10 E Saturn Boulevard, Edwards AFB, California 93524-7680; and Australian Synchrotron Research Program, Advanced Photon Source, Bldg 434, Argonne, Illinois 60439

Received August 27, 2005; Revised Manuscript Received January 6, 2006

ABSTRACT: A series of hybrid organic/inorganic triblock copolymers of polystyrene−butadiene−polystyrene (SBS) grafted with polyhedral oligomeric silsesquioxane (POSS) molecules with different chemical constituents were synthesized by a hydrosilation method. Four POSS macromers, $R'R_7Si_8O_{12}$, were designed to contain a single silane functional group, R′, which was used to graft onto the dangling 1,2-butadienes in the polybutadiene soft block and seven identical organic groups, R. Small-angle X-ray scattering and rheological techniques were used to study the effect of sterically similar, yet electronically different, organic R groups, cyclopentyl (Cp), cyclohexyl (Cy), cyclohexenyl (Cye), and phenyl (Ph), on the morphology of SBS triblock copolymer and the order−disorder transition behavior. It was observed that POSS with phenyl moiety, when grafted to the polybutadiene (PB) phase, appears to show favorable interaction with the polystyrene (PS) phase; effectively, the Ph-POSS is plasticizing the SBS due to an effect whereby the Ph-POSS is at least partially solvated by the PS phase. This causes a significant decrease in the overall lamellae *d* spacing and the order−disorder transition temperature, T_{ODT}, with increasing amounts of Ph-POSS attachment. As we change the POSS moiety to that of Cye, Cy, and Cp, the interaction between POSS-PS weakens, and the *d* spacing and T_{ODT} become less dependent on the amounts of POSS attachment. At the highest POSS loadings investigated (20 wt %), there is a change to a perforated layer morphology, resulting in an increase of T_{ODT} relative to the 10 wt % POSS-grafted copolymers for Cp, Cy, and Cye POSS moieties.

I. Introduction

For a sufficiently high degree of segregation, block copolymers will undergo microphase separation into self-assembled ordered morphologies.[1−20,22] Various approaches to manipulate domain morphology have been explored by researchers over the past 20 years[6−10,13−22] and have led to an important class of engineering polymers often referred to as the thermoplastic elastomers. Hence, the recent interest in nanoreinforced polymers has included the use of "nanomaterials" to further explore the property space of block copolymers.[22,23] One such approach is to append the block copolymers using a well-defined nanostructured chemical to a given segment of the copolymer.[22,24] If these nanosized objects are well dispersed on the length scale comparable to periodicity of block copolymer matrix, one expects the surface chemistry of the nanostructured chemicals and their interactions with different components of the block copolymer to play a significant role in altering the thermodynamics and morphology of the copolymer matrix. Polyhedral oligomeric silsesquioxanes (POSS) are a type of model nanostructured chemical. A fully condensed POSS contains an inorganic Si−O core surrounded with various organic groups useful for tuning the surface chemistry and interaction with the host copolymer matrix. POSS can be either randomly blended or grafted to a particular phase of a copolymer. This enables us to investigate the influence of nanomaterial chemistry on the thermodynamics and morphology of a block copolymer matrix.

In this study, we examine how the host copolymer morphology and its order−disorder transition temperature, T_{ODT}, are affected by the chemistry of grafted nanostructured chemicals. It is known that the addition of solvents or homopolymers to a block copolymer system can change the length scale or lattice spacing of the morphology, the T_{OOT} and T_{ODT}, and possibly the type of morphology. Solvents range from neutral to strongly selective depending on how it preferentially swells each microdomain of the copolymer morphology. Homopolymers that are of type A or B of the AB or ABA copolymers will also exhibit behavior like that of selective solvents in a block copolymer−homopolymer blend. On the basis of our previous work,[22] polystyrene-*block*-polybutadiene-*block*-polystyrene (SBS) triblock copolymer was selected as the model copolymer matrix. SBS was chosen as a host polymer because it is commercially available in narrow molecular weight distributions, and it has been used in a wide range of applications. SBS also has the ability to form various self-assembled morphologies which allow for direct examination of how the insertion of a nanostructured chemical affects the morphology. The model POSS used in this study are inorganic silicon−oxygen cages on the order of a nanometer in size with various organic moieties bonded to the silicon atoms.[25] Four POSS moieties used in this study for grafting to SBS triblocks are all of the formula $R'R_7Si_8O_{12}$. R′ provides a single flexible Si−H linkage for grafting to polybutadiene while four different R groups, cyclopentyl (Cp), cyclohexyl (Cy), cyclohexenyl (Cye), and phenyl (Ph), provide a range of sterically similar, yet electronically different, organic moieties for investigating the tunability of the POSS. Cp and

[†] Michigan State University.
[‡] Air Force Research Laboratory.
[§] Advanced Photon Source.
* To whom correspondence should be addressed. E-mail: leea@egr.msu.edu.

10.1021/ma0518813 CCC: $33.50
Published on Web 02/03/2006

Cy-POSS are saturated, Cye is unsaturated, and Ph is aromatic. On the basis of their electronic structure, it might be assumed that Cp and Cy-POSS will have a greater affinity for PB than PS whereas Ph-POSS will have a greater affinity toward PS. Cye-POSS, having an electronic structure between Cy and Ph, will likely have relative compatibilities between the two as well. In addition, because the molecular weight and size of each POSS are nearly identical, any differences found between POSS-grafted SBS copolymers will be directly attributable to R-group/SBS compatibility.

II. Experimental Section

General Information in Synthesis. Toluene was dried by passage through activated alumina columns,[26] 1,4-bis(dimethylsilyl)-benzene was distilled under dynamic vacuum prior to use, and Karstedt catalyst (solution in xylenes) was purchased from Aldrich. The SBS used for this study was Vector 6241 obtained from Dexco Polymers LP, a Dow/ ExxonMobil Venture. According to the manufacturer, it is a pure, linear symmetric triblock copolymer containing less than 1% diblock and has 43 wt % polystyrene. The number-average molecular weight is 71 kDa, and the weight-average molecular weight is 72 kDa. This gives SBS respective degrees of polymerization of approximately 150−750−150. SBS triblock copolymer was dried at 60 °C overnight under vacuum, and all initial POSS trisilanol materials were obtained from Hybrid Plastics Inc. All NMR spectra were collected on either a Bruker 300 or 400 MHz instrument and obtained from $CDCl_3$ solutions. ^1H, ^{13}C, and ^{29}Si NMR spectra (reported in ppm using the δ scale) were referenced to residual $CHCl_3$ at 7.26 ppm, to $CDCl_3$ at 77.0 ppm, and to external $SiMe_4$ at 0 ppm, respectively. HPLC were obtained on a HP 1090 liquid chromatograph by injecting 10 μL of a 5 ppt sample onto a poly(vinyl alcohol)−silica gel column and eluting at 1 mL/min using a 5 vol % THF/95 vol % cyclohexane mobile phase and a Varex MKIII evaporative light scattering detector. Molecular weights were determined using gel permeation chromatography and a combination of refractive index and multi-angle laser-light scattering measurements on a Wyatt Technology Corp. DAWN spectrometer.

Synthesis of Hydride Reagent: $Cl_3Si(CH_2)_3SiMe_2(C_6H_4)(SiMe_2H)$. Under a dry nitrogen atmosphere, allyl-$SiCl_3$ (6.55 g, 37.3 mmol) was slowly added over ∼30 min to a ∼7-fold excess of $HSiMe_2C_6H_4SiMe_2H$ (50 g, 257 mmol) activated with 5 drops of Karstedt catalyst solution. The exothermic reaction became hot to the touch toward the end of the addition. After stirring for a further hour, the mixture was distilled under full dynamic vacuum. Unreacted $HSiMe_2C_6H_4SiMe_2H$ (42 g) distilled first at 35 °C and was isolated for future reactions. A second fraction, collected as the temperature ramped to 93 °C, was a mixture of product and $HSiMe_2C_6H_4SiMe_2H$. The third fraction contained pure product (13.27 g, 35.9 mmol), isolated in 96% yield. ^1H NMR (δ, ppm, 400 MHz): 7.67 (mult, 2H, aromatic), 7.63 (mult, 2H, aromatic), 4.56 (sept, 1H, hydride, $^1J_{Si-H} = 3.6$ Hz), 1.77 (mult, propyl CH_2), 1.56 (mult, 2H, propyl CH_2), 1.02 (mult, 2H, propyl CH_2), 0.46 (doublet, 6H, $SiMe_2$, $^1J_{Si-H} = 3.6$ Hz), 0.41 (s, 6H, $SiMe_2$). ^{13}C {^1H} NMR (δ, ppm, 100.6 MHz): 139.72, 138.30, 133.41, 132.91 (aromatic); 28.21, 18.70, 17.29 (propyl CH_2); −3.16, −3.83 ($SiMe_2$). ^{29}Si {^1H} NMR (δ, ppm, 79.5 MHz): +12.51 (1Si, $SiCl_3$), −3.20 (1Si, $SiMe_2$), −16.87 (1Si, $SiMe_2H$).

Synthesis of Cyclopentyl-POSS-Hydride: $(c\text{-}C_5H_9)_7[Si_8O_{12}]((CH_2)_3SiMe_2(C_6H_4)(SiMe_2H))$. Under a dry nitrogen atmosphere, a THF solution (10 mL) of $Cl_3Si(CH_2)_3SiMe_2(C_6H_4)(SiMe_2H)$ (2.218 g, 6.00 mmol) was added over 10 min to a well-stirred THF (50 mL) solution of POSS-trisilanol, $(c\text{-}C_5H_9)_7[Si_7O_{11}](OH)_3$ (5.000 g, 5.71 mmol) and triethylamine (1.91 g, 18.85 mmol). After stirring overnight, the triethylammonium hydrochloride byproduct was separated by filtration, and the THF solution was evacuated to dryness. Under air, this solid was extracted with diethyl ether and then washed first with distilled water and then with saturated brine. The organic layer was separated from the aqueous and dried with $MgSO_4$ for 1 h. After filtration, the clear ether solution was evacuated to near dryness and then added dropwise to well-stirred methanol. The product precipitated as a fine white powder. After stirring overnight, pure product was isolated by filtration and dried under a steady stream of nitrogen gas to give an 83% yield (5.39 g, 4.74 mmol) of product. ^1H NMR (δ, ppm, 400 MHz): 7.53 (mult, 4H, aromatic), 4.45 (sept, 1H, hydride, $^1J_{Si-H} = 3.6$ Hz), 1.78 (mult, 14H, cyclopentyl CH_2), 1.54 (mult, 44H, cyclopentyl CH_2, propyl CH_2), 1.02 (mult, 7H, cyclopentyl CH), 0.88 (mult, 2H, propyl CH_2), 0.71 (mult, 2H, propyl CH_2), 0.37 (doublet, 6H, $SiMe_2$, $^1J_{Si-H} = 3.6$ Hz), 0.27 (s, 6H, $SiMe_2$). ^{13}C {^1H} NMR (δ, ppm, 100.6 MHz): 140.73, 137.75, 133.20, 132.93 (aromatic); 27.33, 27.30, 27.02, 26.98 (cyclopentyl CH_2); 22.25 (cyclopentyl CH); 19.10, 17.51, 16.31 (propyl CH_2); −3.14, −3.89 ($SiMe_2$). ^{29}Si {^1H} NMR (δ, ppm, 79.5 MHz): −3.40 (1Si, $SiMe_2$), −17.02 (1Si, $SiMe_2H$), −66.25 (4Si, Si-cyclopentyl), −66.41 (3Si, Si-cyclopentyl), −66.57 (1Si, Si-propyl). HPLC gave a single peak.

Synthesis of Cyclohexyl-POSS-Hydride: $(c\text{-}C_6H_{11})_7[Si_8O_{12}]((CH_2)_3SiMe_2(C_6H_4)(SiMe_2H))$. The same procedure was used to make the cyclohexyl-substituted POSS derivative, isolated in 88% yield. ^1H NMR (δ, ppm, 400 MHz): 7.51 (mult, 4H, aromatic), 4.42 (sept, 1H, hydride, $^1J_{Si-H} = 3.6$ Hz), 1.73 (mult, 35H, cyclohexyl CH_2), 1.51 (mult, 2H, propyl CH_2), 1.24 (mult, 35H, cyclohexyl CH_2), 0.86 (mult, 2H, propyl CH_2), 0.75 (mult, 7H, cyclohexyl CH), 0.69 (mult, 2H, propyl CH_2), 0.34 (doublet, 6H, $SiMe_2$, $^1J_{Si-H} = 3.6$ Hz), 0.25 (s, 6H, $SiMe_2$). ^{13}C {^1H} NMR (δ, ppm, 100.6 MHz): 140.75, 137.78, 133.21, 132.91 (aromatic); 27.51, 27.47, 26.91, 26.85, 26.63 (cyclohexyl CH_2); 23.15 (cyclohexyl CH); 19.15, 17.60, 16.27 (propyl CH_2); −3.15, −3.90 ($SiMe_2$). ^{29}Si {^1H} NMR (δ, ppm, 79.5 MHz): −3.43 (1Si, $SiMe_2$), −17.03 (1Si, $SiMe_2H$), −66.47 (1Si, Si-propyl), −68.38 (4Si, Si-cyclohexyl), −68.56 (3Si, Si-cyclohexyl). HPLC gave a single peak.

Synthesis of Cyclohexenyl-POSS-Hydride: $(c\text{-}C_6H_9)_7[Si_8O_{12}]((CH_2)_3SiMe_2(C_6H_4)(SiMe_2H))$. The same procedure was used to make the cyclohexenyl-substituted POSS derivative, isolated in 82% yield. ^1H NMR (δ, ppm, 400 MHz): 7.50 (mult, 4H, aromatic), 5.72 (mult, 14H, cyclohexenyl CH═CH), 4.45 (sept, 1H, hydride, $^1J_{Si-H} = 3.6$ Hz), 2.03 (mult, 28H, cyclohexenyl CH_2), 1.85 (mult, 7H, cyclohexenyl CH_2), 1.46 (mult, 9H, cyclohexenyl CH_2, propyl CH_2), 1.01 (mult, 7H, cyclohexenyl CH), 0.85 (mult, 2H, propyl CH_2), 0.71 (mult, 2H, propyl CH_2), 0.34 (doublet, 6H, $SiMe_2$, $^1J_{Si-H} = 3.6$ Hz), 0.24 (s, 6H, $SiMe_2$). ^{13}C {^1H} NMR (δ, ppm, 100.6 MHz): 140.52, 137.80, 133.19, 132.84 (aromatic); 127.28, 127.26, 127.03, 126.99 (cyclohexenyl CH═CH); 25.40, 25.38, 24.96, 22.52 (cyclohexenyl CH_2); 18.50, 18.47 (cyclohexenyl CH); 19.16, 17.52, 16.11 (propyl CH_2); −3.20, −3.94 ($SiMe_2$). ^{29}Si {^1H} NMR (δ, ppm, 79.5 MHz): −3.45 (1Si, $SiMe_2$), −17.02 (1Si, $SiMe_2H$), −66.16 (1Si, Si-propyl), −67.65 (4Si, Si-cyclohexenyl), −67.89 (3Si, Si-cyclohexenyl). HPLC gave a single peak.

Synthesis of Phenyl-POSS-Hydride: $(C_6H_5)_7[Si_8O_{12}]((CH_2)_3SiMe_2(C_6H_4)(SiMe_2H))$. Because a phenyl-substituted POSS trisilanol reacts with triethylamine, a slightly different procedure was used to make this derivative. Under a dry nitrogen atmosphere, a THF solution (10 mL) of triethylamine (1.434 g, 14.17 mmol) was slowly added over 20 min to a well-stirred THF (50 mL) solution of POSS-trisilanol, $(C_6H_5)_7[Si_7O_{11}](OH)_3$ (4.000 g, 4.30 mmol) and $Cl_3Si(CH_2)_3SiMe_2(C_6H_4)(SiMe_2H)$ (1.668 g, 4.51 mmol). After stirring overnight, the triethylammonium hydrochloride byproduct was separated by filtration, and the THF solution was evacuated to dryness. Under air, this solid was extracted with diethyl ether and washed first with distilled water and then with saturated brine. The organic layer was separated from the aqueous and dried with $MgSO_4$ for 1 h. After filtration, the clear ether solution was evacuated to near dryness and then added dropwise to well-stirred methanol. The product precipitated as a fine white powder. After stirring overnight, pure product was isolated by filtration and dried under a steady stream of nitrogen gas to give an 84% yield (4.30 g, 3.61 mmol) of product. ^1H NMR (δ, ppm, 400 MHz): 7.76 (mult, 14H, aromatic), 7.48 (mult, 11H, aromatic), 7.38 (mult, 14H, aromatic), 4.42 (sept, 1H, hydride, $^1J_{Si-H} = 3.6$ Hz), 1.63 (mult, 2H, propyl CH_2), 0.95 (mult, 2H, propyl CH_2), 0.88 (mult, 2H, propyl CH_2),

0.32 doublet, 6H, $SiMe_2$, $^1J_{Si-H} = 3.6$ Hz), 0.19 (s, 6H, $SiMe_2$). ^{13}C {^1H} NMR (δ, ppm, 75.5 MHz): 140.56, 137.79, 133.27, 132.90 (C_6H_4); 134.19, 134.15, 130.74, 130.46, 130.27 (C_6H_5); 19.17, 17.45, 16.16 (propyl CH_2); −3.17, −3.89 ($SiMe_2$). ^{29}Si {^1H} NMR (δ, ppm, 59.6 MHz): −3.61 (1Si, $SiMe_2$), −17.22 (1Si, $SiMe_2H$), −65.25 (1Si, Si-propyl), −78.23 (4Si, Si-phenyl), −78.71 (3Si, Si-phenyl). HPLC gave a single peak.

Example Grafting Reaction of 10 wt % POSS-Hydride to SBS Polymer. Under a dry nitrogen atmosphere, a toluene solution (10 mL) containing 2 drops of Karstedt catalyst solution and phenyl-POSS-hydride (1.20 g) was added to a well-stirred solution of SBS (4.80 g) in dry toluene (170 mL) and heated to 60 °C. After stirring overnight, an aliquot was removed and checked by ^1H NMR to ensure complete consumption of the POSS-hydride. Platinum catalyst was removed by stirring several hours with silica followed by filtration. The filtrate was then added dropwise to well-stirred methanol (250 mL) to precipitate the grafted polymer. The precipitated polymer was dried in a vacuum oven at 50 °C overnight to yield 5.76 g of product. All the grafted polymers were prepared in this same manner.

Sample Preparation. Samples were prepared in the form of solvent-cast films measuring ~0.3 mm in thickness. The copolymer samples were dissolved in a toluene, a neutral solvent, in a 3.0 wt % concentration. Approximately 0.5 wt % antioxidant (relative to the polymer) was also added to the solution to reduce degradation at high temperatures. The solvent was then allowed to evaporate on glass at 20 °C over a period of 3 days. The films were removed from the glass and were then annealed under vacuum at 60 °C for 7 days.

Small-Angle X-ray Scattering (SAXS). SAXS measurements were performed at beamline 15ID-D (ChemMatCARS) in the Advanced Photon Source (APS) at Argonne National Laboratory. The energy of radiation used for the experiments was 8.27 keV ($\Delta E/E \approx 10^{-4}$), which corresponds to an X-ray wavelength of 1.50 Å. SAXS images were collected using a two-dimensional Bruker 6000 CCD X-ray detector with a 1024 × 1024 pixel array on a 94 × 94 mm area. The sample to detector distance was ~1900 mm and was calibrated using silver behenate.

Two types of SAXS experiments were performed: isothermal and temperature ramp. The isothermal experiments were used to examine how the equilibrium block copolymer morphology is affected by the type and amount of POSS grafted at selected temperatures. The samples were heated in an electric heating cell which consisted of a resistance heating element inside an enclosed 150 cm^3 volume. The heating cell had two Kapton windows which allowed the X-ray beam to pass through the cell with little scattering and attenuation while containing the internal environment. A flow of nitrogen gas was used to both stabilize the temperature within the heating cell and reduce the degradation of the samples. All isothermal scans were performed after a 5 min equilibration period. Data collection was performed over a period of several minutes by taking 1 s exposures at several points on a two-dimensional raster covering a 3 mm by 3 mm area of the sample film. This was done to reduce the beam damage on the sample and to achieve better SAXS profile statistics by ensuring the sample morphology reached equilibrium and to examine errors due to possible temperature variations and morphological variations within the bulk material. Temperature ramp experiments were performed to examine the T_{ODT} of each block copolymer sample. Samples were heated to 150 °C and held isothermally for 5 min before increasing temperature at a rate of 2 °C/min. A flow of dry nitrogen gas was used to both stabilize the temperature within the heating cell and reduce sample degradation. T_{ODT} was calculated by examining the peak width as a function of temperature.

The 2-D SAXS images, like that in Figure 1a, were through views of the cast films (i.e., the film surface is normal to the incident X-ray beam). The 2-D images show concentric, uniform intensity rings which indicate that the solvent-casting process results in a random microdomain orientation analogous to a metallic polycrystal in the plane of the film surface. The 2-D SAXS images are integrated 360° azimuthally to give the SAXS profiles shown in Figure 1b. The SAXS profiles show the intensity of scattered radiation vs the magnitude of the scattering vector, q

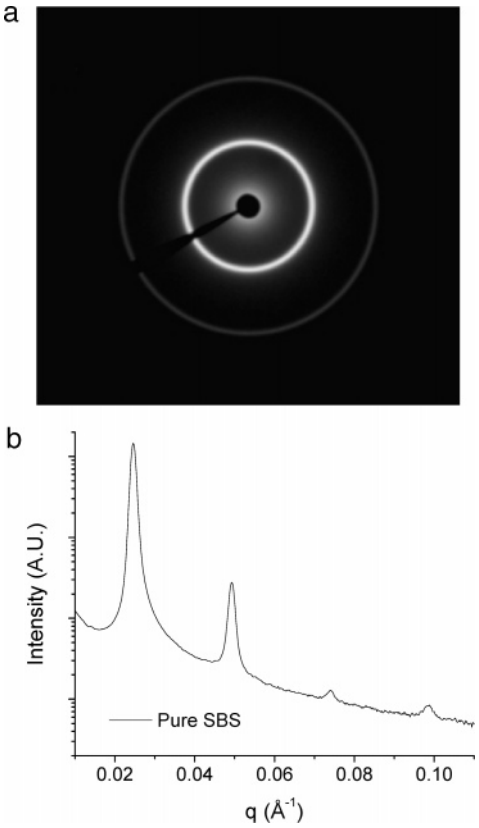

Figure 1. (a) Two-dimensional SAXS pattern of pure SBS at 130 °C. (b) SAXS intensity vs scattering vector, q, based on 360° azimuthally integration of 2-D image as depicted in (a).

$$q = \frac{4\pi \sin\theta}{\lambda} \tag{1}$$

There are three features of these SAXS profiles that will be of interest in the results and discussion: the relative position and intensity of the higher order peaks which is defined by the type of morphology, the primary peak width which is related to the local order of the morphology, and the primary peak position which determines the d spacing. To determine precise changes in peak position and intensity, peak statistics were calculated by fitting curves using nonlinear least-squares regression analysis. The fitting function included a Gaussian peak of the form $A \exp[-(x - q^*)^2/b]$ and a background of the form $\sum_{i=0}^{4} A_i x^{-i}$ where $A_i > 0$. For the Gaussian peak, A is the amplitude of the peak, $\Gamma = 2\sqrt{b\ln 2}$ is the full width at half-maximum of the peak, and q^* is the location of the peak maximum. By substituting Bragg's law into eq 1

$$q^* = 2\pi/d \tag{2}$$

where d is the periodicity or d spacing. A Gaussian peak was used for the fit because it well-represented the peak shape. There was an underestimation of the peak width/amplitude near the base of the peak, but this was small and symmetric and did not affect the comparison of peak width statistics across a copolymer series. The $A_i x^{-i}$ form of the background fitting was used because of its excellent rate of convergence compared to exponentials and because it followed the monotonically decreasing background. The background ranges from 1% to 8% of the primary peak height on a linear scale. The coefficient of determination, R^2, was better than 0.995 over the entire peak profile for a domain of 40 data points, which suggests a good fit to the data.

Rheological Characterization. Rheological testing was performed using a TA Instruments AR2000 rheometer with direct

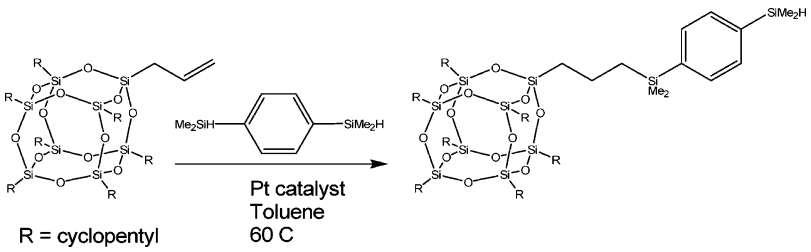

Figure 2. Old synthesis route for cyclopentyl-POSS-hydride.[22]

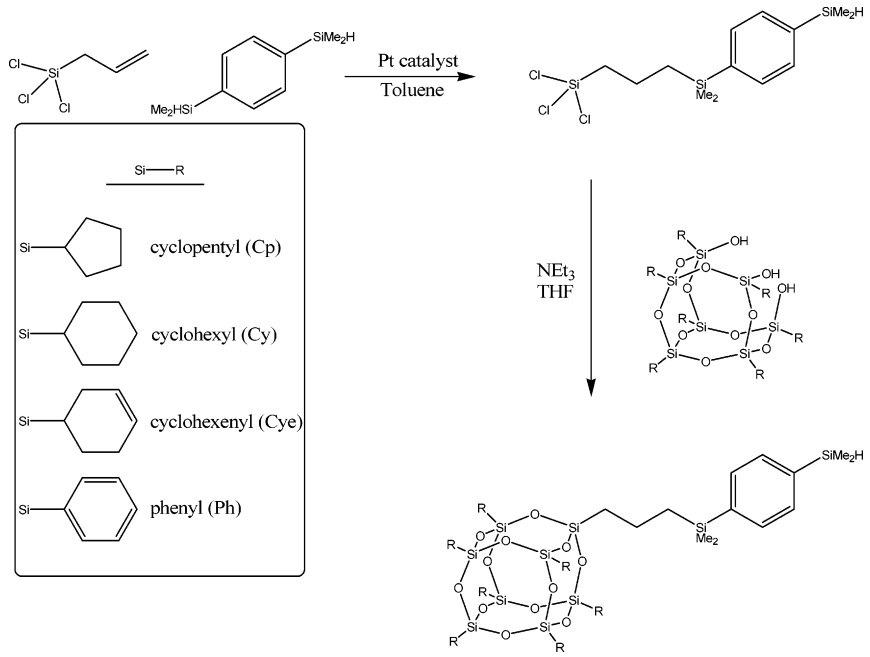

Figure 3. New synthesis route of POSS-hydrides.

strain-control mode. The rheometer is equipped with an electric heater with dry N_2 purging (purging rate is 12 mL/min); the temperature in the testing chamber is monitored with an embedded thermocouple within the bottom tool of the rheometer, which is in direct contact with the sample. Parallel plate geometry with diameter of 25 mm and gap of 0.2 mm was used for all measurements obtained in this study. The fixture was preheated to the initial testing temperature of 150 °C and lowered to obtain the zero-gap reference point. The disk-shaped specimen was then placed in the rheometer, and the top fixture was slowly lowered to the preset gap of 0.2 mm with minimal normal force. Sample was annealed at 150 °C for 5 min prior to rheological testing. To determine order−disorder transition temperature, T_{ODT}, the sample was subjected to a fixed, small-strain oscillatory shear test with strain amplitude of 2% and oscillatory frequency of 1 rad/s at a heating rate of 2 °C/min. Software as provided by TA Instruments Inc. was used to determine the temperature-dependent storage modulus $G'(\omega)$ which was used for T_{ODT} analysis.

III. Results and Discussion

New Approach to the Synthesis of POSS-Hydrides. One of the simplest methods of modifying a polymer with a polyhedral oligomeric silsesquioxane (POSS) type molecule without changing the backbone degree of polymerization is to make use of a platinum-catalyzed hydrosilation reaction.[27] The polymer must contain dangling olefins, and the POSS must have a reactive silane. Previously, we reported the synthesis of a cyclopentyl-derivatized POSS-hydride that grafts well onto SBS materials.[22] We now report an improved synthesis of this hydride as well as other derivatives. The older synthesis (shown in Figure 2) used a hydrosilation reaction of a POSS-allyl with a 10-fold excess of 1,4-bis(dimethylsilyl)benzene in toluene solution at 60 °C. However, a trace amount of bis-hydrosilated product was present and proved to be difficult to separate from the product.

An improved synthesis route is shown Figure 3. We first react allyltrichlorosilane with a 10-fold excess of 1,4-bis(dimethylsilyl)benzene using platinum-catalyzed hydrosilation and isolate a pure trichlorosilane with vacuum distillation. Unreacted 1,4-bis(dimethylsilyl)benzene is also isolated and reused in subsequent reactions. The trichlorosilane is then reacted with any POSS-triol in a second reaction to form a variety of POSS-hydrides in excellent yield and purity. The typical synthetic procedure is to slowly add the trichlorosilane to a THF solution of a POSS-trisilanol and triethylamine; however, for the phenyl-substituted POSS derivative, it is necessary to change the order of addition. Slow addition of the triethylamine to a THF solution of trisilanol and chlorosilane is required because triethylamine catalyzes the decomposition of phenyl-POSS triol due to its increased acidity relative to alkyl-substituted POSS triols.[28]

The grafting of POSS-hydride onto a styrene−butadiene−styrene triblock is illustrated in Figure 4. The SBS triblock polymer is a narrow disperse 71 000 g/mol ($M_w/M_n = 1.02$) material with a butadiene to styrene molar ratio of 2.54:1.00 containing ~150 styrene units on either end of a block of 750 butadiene units. The butadiene and styrene phases are nearly equivalent, with 57 wt % of the material being made from butadiene and 43 wt % from styrene. ^{1}H NMR spectroscopy reveals that the polybutadiene block contains ~9% 1,2-polymerized butadiene; the remaining 91% is 1,4-polymerized butadiene containing unequal amounts of *trans*- and *cis*-olefins; there is significantly more trans than cis, but we did not quantify

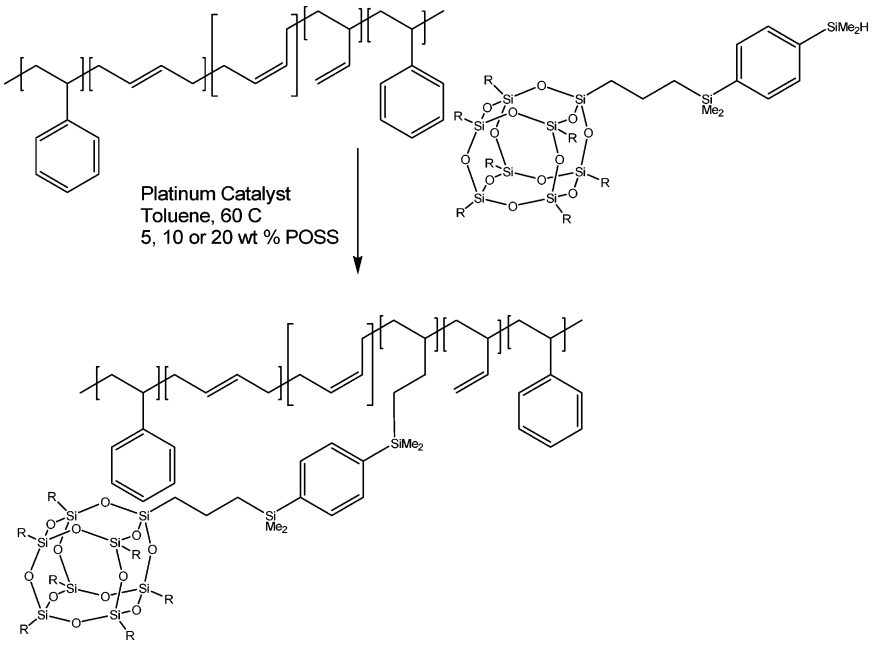

Figure 4. Grafting of a POSS-hydride to SBS triblock. Note that the double bonds in the butadiene block are a random mixture of mostly internal cis and trans with ~9% dangling from the main polymer backbone. The dangling double bonds are reactive to hydrosilation chemistry.

this difference because of inadequate resolution on a 400 MHz NMR instrument.[29] We assume that there is a random distribution of these three units within the polybutadiene block. Only the 9% dangling 1,2-polymerized butadiene is available for hydrosilation reactions. On average, each polymer chain contains 67 of these reactive dangling olefins. Theoretically, we could add between 1 and 67 POSS-hydrides to each chain; this is equivalent to a range from 1 to 53 wt % phenyl-POSS. For this study, we grafted 5, 10, and 20 wt % POSS to the base SBS triblock; this translates to an *average* of 3, 7, or 15 POSS cages grafted to each chain. Of course, some chains will have less (or even no POSS) and some will have more than this average value.

The grafting of the POSS-hydride to the SBS polymer is conveniently followed by ^{1}H NMR spectroscopy (Figure 5). The $Si(CH_3)_2H$ unit has diagnostic resonances with a hydride septet near 4.5 ppm and a silylmethyl doublet at 0.37 ppm. As this moiety reacts with 1,2-polymerized butadiene (multiplets centered at 5.57 and 4.98), all these signals are reduced in intensity and a single $Si(CH_3)_2$ signal grows near 0.26 ppm.

Effect of POSS Moieties on Morphology. The morphology of POSS-grafted SBS triblock copolymers was investigated using the small-angle X-ray scattering (SAXS) technique. SAXS not only offers a nondestructive evaluation over a large volume of material but also enables us to monitor changes in morphology as a function of temperature. Transmission electron microscopy (TEM) is another common technique used to investigate morphology of block copolymers.[23c] However, there are several possible problems associated with this technique for SBS with nanoscopic inclusions. First, it is common practice to stain SBS with OsO_4 to distinguish different segments of the block copolymer. The chemical nature of POSS will affect the reaction between OsO_4 and butadiene, which may alter the original morphology. Without staining, there will not be enough electronic contrast to investigate any morphology present. The relatively low volume fraction of POSS present in the butadiene segments will not provide enough contrast to reveal any useful morphological information. Another issue with TEM is the small sampling volume. The TEM micrograph may not best represent the bulk copolymer, especially when used to study the effect of POSS-grafted copolymers.

The 2-D SAXS profiles in Figure 6a−d show the integrated intensity as a function of scattering vector, q, for pure SBS along with 5, 10, and 20 wt % at 130 °C for each POSS moiety used here. The relative location of the peaks is determined by the morphology. The pure SBS has peak spacings of q^*, $2q^*$, $3q^*$, and $4q^*$ where q^* is the position of the first and most intense scattering peak, referred to as the primary peak. The observed integer spacings are equivalent to the structure factor of a lamellar morphology which is predicted for the 43% polystyrene weight fraction. The 5 and 10 wt % POSS loading of each moiety show little qualitative change from the pure SBS. The relative position and intensity of the higher order peaks do not change, which shows that the lamellar morphology is preserved. The presence and preserved intensity of the second-, third-, and fourth-order peaks suggest that the long-range periodicity of the lamellae is maintained at these grafted POSS loadings. For samples with 20 wt % loadings the second-order peak, though still present, has significantly diminished intensity, and there are no observed third- or fourth-order peaks. This suggests for Dexco 6241 SBS, when grafted with 20 wt % POSS molecules, the basic form of the lamellar morphology exists, but the lamellae have become disrupted. These changes in the SAXS profiles are consistent with a perforated layer morpology.[30] The addition of POSS to SBS alters the volume ratio of styrene and butadiene domains, and since the POSS is grafted to the butadiene block, it will act like a selective solvent having a preference to the PB. However, the degree of selectivity will depend on the chemical substituent of POSS used. Other than the order−disorder transition, no other morphological phase transitions were observed for any of the POSS-grafted SBS investigated.

The width of the primary peak for a copolymer specimen is affected by a number of factors. For undeformed materials, some of the factors that contribute to peak broadening in the lamellar morphology are variance in lamellar thickness, a limited number of lamellae in the diffracting stacks (i.e., small domain size), defects of lamellae at domain boundaries, and lamellae interface

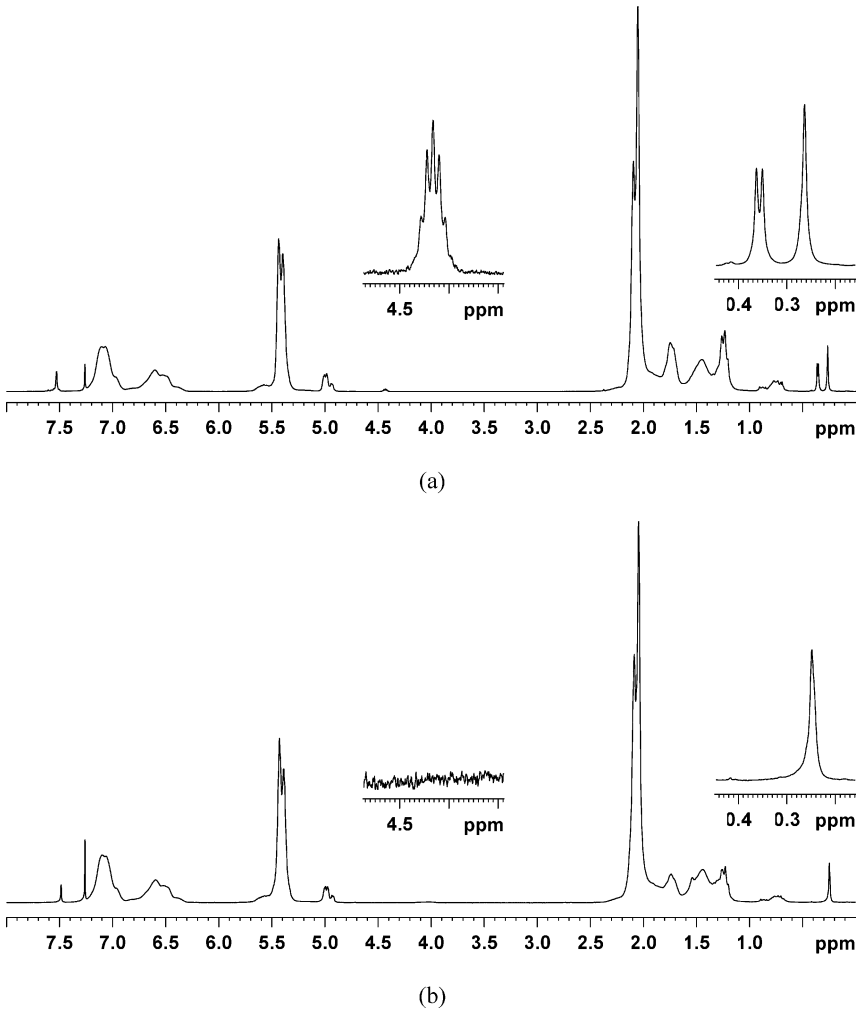

Figure 5. ^{1}H NMR spectra of **(a)** 20 wt % POSS-hydride and 80 wt % SBS copolymer with no Pt catalyst and **(b)** 20 wt % POSS hydride grafted to SBS. The insets show how the hydride resonance disappears and silylmethyl region changes before and after grafting.

fluctuations (i.e., curvature at the styrene−butadiene interface). Thus, the peak width can be used to quantify the relative local order and/or defects of the morphology.

Figure 7 shows the peak width for each POSS moiety at 150 °C as a function of POSS loading. The 5 and 10 wt % grafted samples show only a small amount of broadening for all POSS moieties, but broadening becomes more significant at 20 wt %. At this high POSS loading, the noticeable increases in peak width can again be associated with the transition to a perforated layer morphology. The peak width data, coupled with the observation of high-order diffraction peaks discussed earlier, suggests that grafting of up to 10 wt % phenyl-POSS causes only negligible changes in the qualitative morphology as a whole. Both local ordering and long-range periodicity are maintained to a large degree. With the increased POSS grafting of 20 wt %, the morphology becomes considerably disturbed as noted by the significant peak broadening along with the reduced intensity and disappearance of higher order peaks.

Another possible factor which may contribute to the peak broadening is the altered molecular weight distribution and polydispersity by grafting POSS on a nearly monodisperse SBS triblock copolymer. Assuming the chemical attachment of POSS during the grafting reaction is random (i.e., each 1−2 PB reaction site is equally likely to undergo POSS attachment throughout the reaction), the distribution of POSS per chain would be nearly binomial which has a variance and thus will contribute to the overall polydispersity. This means one can expect that the grafted POSS-copolymer system will possess an increased variance and polydispersity.

To illustrate this effect, we listed the molecular weight analysis of SBS grafted with varying amounts of phenyl-POSS in Table 1. The polydispersity due to the POSS attachment may account for some of the peak width and qualitative morphological changes, but it is unlikely that it accounts for the entire peak broadening. Compared to the overall SBS molecular weight, this variance is small but nonetheless may still be a factor. It is also assumed that all moieties are affected similarly. One observation that supports this is the ability to form well-defined self-assembled morphologies at 10 wt % POSS grafting. To have this long-range periodicity, the polymer must be sufficiently narrow in molecular weight.

The differences in peak width across POSS moiety are relatively small. In fact, other than the 20 wt % cyclopentyl (Cp) loading all the data are within experimental error. This suggests that the observed changes in the qualitative lamellar morphology may be inherent to the grafting of POSS and not the chemical nature of the POSS moiety grafted. The small changes in peak width across POSS moiety match qualitatively with the SAXS profile comparison.

The length of the lamellar periodicity, the *d* spacing, is inversely proportional to q^* (eq 2), the position of the first-order peak. Parts a and b of Figure 8 show the *d* spacing at 130 and 150 °C for the lamellar morphology with the Cp, Cy, Cye, and Ph-POSS moieties, respectively. At both temperatures

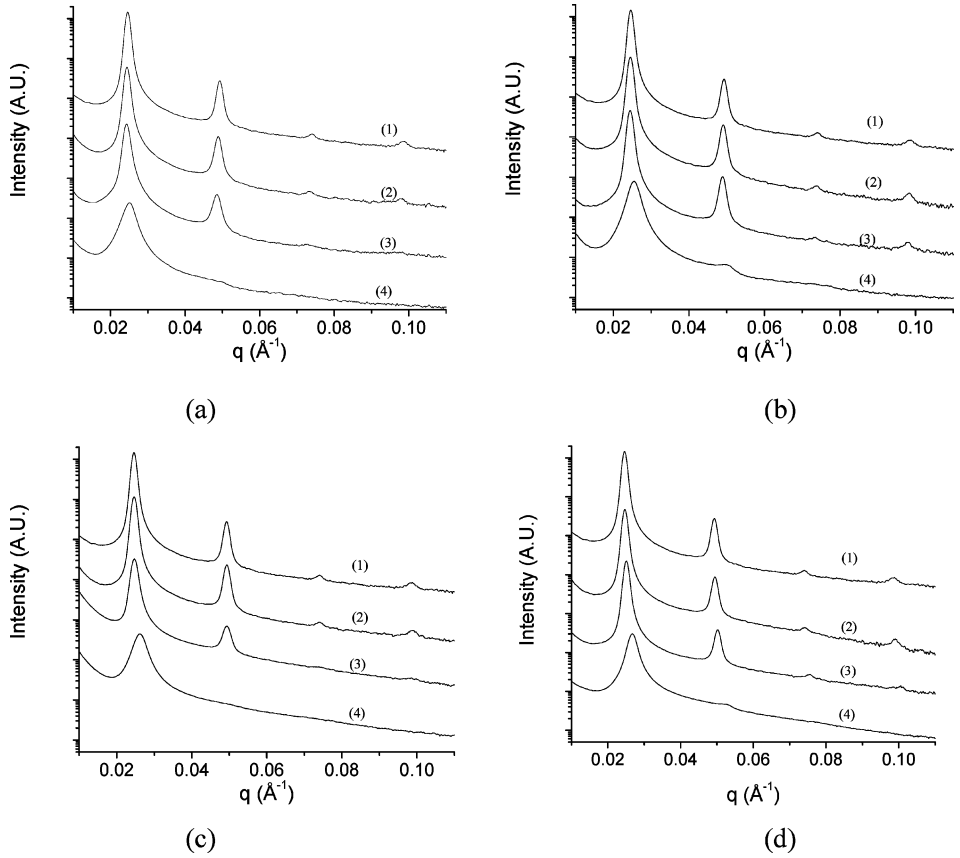

Figure 6. Integrated SAXS intensity vs scattering vector, *q*, for SBS triblock copolymers grafted with different moieties of POSS macromers: (a) cyclopentyl, Cp, moiety POSS is used and (1) SBS control with no POSS, (2) 5 wt % POSS, (3) 10 wt % POSS, (4) 20 wt % POSS; (b) cyclohexyl, Cy, moiety POSS is used and (1) SBS control with no POSS, (2) 5 wt % POSS, (3) 10 wt % POSS, (4) 20 wt % POSS; (c) cyclohexenyl, Cye, moiety POSS is used and (1) SBS control with no POSS, (2) 5 wt % POSS, (3) 10 wt % POSS, (4) 20 wt % POSS; and (d) phenyl, Ph, moiety POSS is used and (1) SBS control with no POSS, (2) 5 wt % POSS, (3) 10 wt % POSS, (4) 20 wt % POSS.

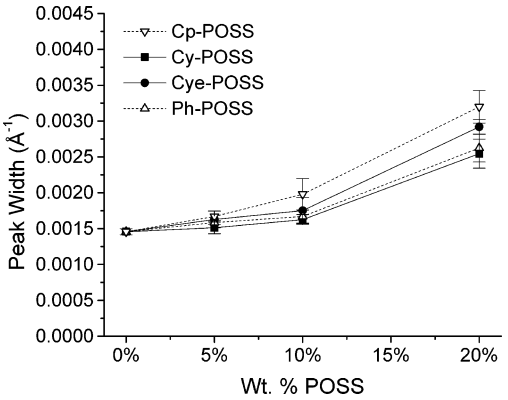

Figure 7. First-order peak width at half-maximum vs varying amounts of POSS with specified moiety of POSS as indicated: (▽) cyclopentyl, Cp, POSS; (■) cyclohexenyl, Cy, POSS; (●) cyclohexenyl, Cye, POSS; (△) phenyl, Ph, POSS.

Table 1. GPC Data for Pure and Ph-POSS-Grafted SBS[a]

wt % POSS	M_w (kDa)	M_n (kDa)	PDI
0	72	71	1.02
5	76	74	1.03
10	78	76	1.03
20	100	93	1.08

[a] Weight percent of POSS is determined by integration of NMR signals. M_n and M_w are number-average and weight-average molecular weights, respectively. PDI is the polydispersity index (M_w/M_n).

significant POSS moiety and grafting fraction effects are observed. In general, we observed a decrease in *d* spacing with increasing amounts of POSS attachment. The 5 wt % data show the smallest decrease in *d* spacing where most of the differences are within experimental error. At 10 wt %, the *d* spacing decreases further for the Cye and Ph moieties while the Cp and Cy *d* spacings remain unchanged. At the highest loading of 20 wt % the *d* spacing drop is significantly greater for all but the Cp-POSS, which remains nearly unchanged. Similar analysis was performed at 150 °C, and the trend is similar which is expected.

The magnitude of the *d* spacing change is strongly influenced by the POSS functionality. Cp-POSS has no statistical change at either temperature. Of the remaining moieties, Cy has the smallest change and Ph-POSS has the greatest change, while Cye-POSS lies in between. In the case of the Cy, Cye, and Ph moieties, the *d* spacing decreases, which results in an increased specific interfacial surface area for the morphology. This suggests a lesser degree of segregation between phase-separated domains, or decreases in the χ-parameter, for these grafted systems. The Cp-POSS samples show almost no change in *d* spacing, so the specific interfacial area remains unchanged. This suggests that the Cp-POSS is completely PB selective in this temperature range. For Cy-POSS, very little changes in *d* spacing are observed at 5 and 10 wt % similar to the Cp data, but at higher loading of POSS there is a drop in *d* spacing. This is attributed to a known compatibility difference between Cp-POSS and Cy-POSS with PS.[25] The better compatibility between Cy-POSS and PS effectively reduces the χ-parameter, causing a greater drop in *d* spacing. For SBS grafted with Ph-POSS, the observed drop in *d* spacing occurs at the lower POSS loadings. The Ph-POSS and the PS repeat units of the block copolymer possess aromatic moieties while PB does not, which

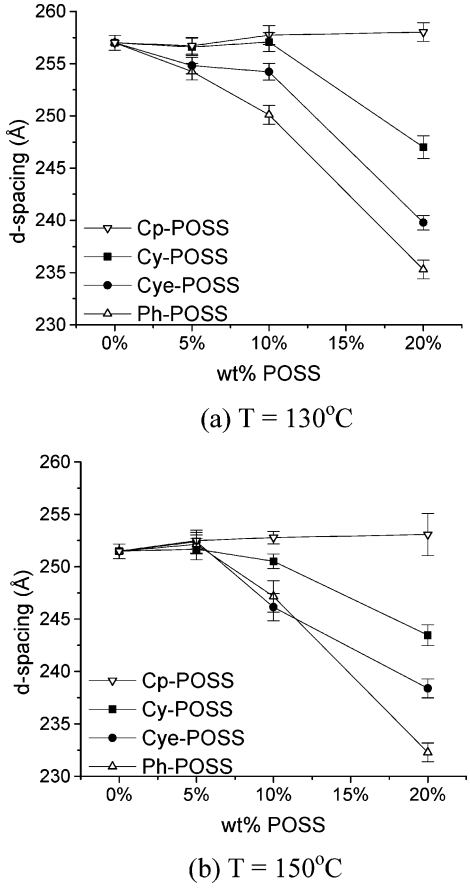

Figure 8. *d*-spacing of SBS triblock copolymer grafted with varying amounts of specified moiety of POSS: (▽) cyclopentyl, Cp, POSS; (■) cyclohexenyl, Cy, POSS; (●) cyclohexenyl, Cye, POSS; (△) phenyl, Ph, POSS; at different temperatures (a) $T = 130$ °C and (b) $T = 150$ °C.

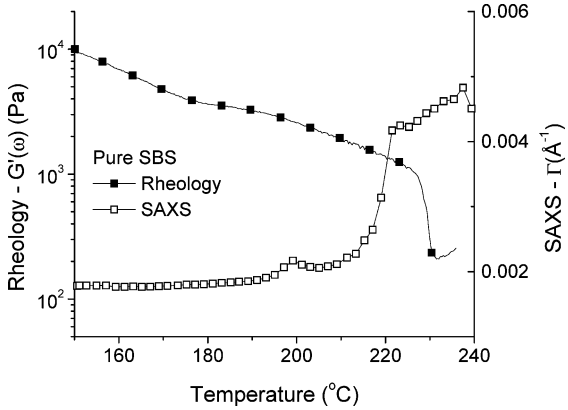

Figure 9. Rheological behavior as represented by the storage modulus, $G'(\omega)$, and SAXS profile as represented by the full width at the half-maximum of the first-order peak, Γ, at the order−disorder region for pure SBS.

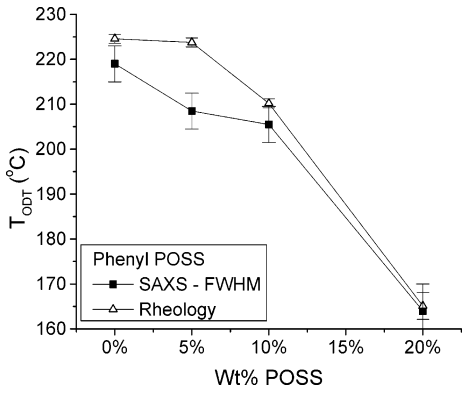

Figure 10. Comparison T_{ODT} as obtained between rheological and SAXS measurements for Ph moiety of POSS.

suggests that the Ph-POSS would have a greater affinity to the PS phase. The unsaturated Cye-POSS has more of a neutral affinity, and as expected its data lie between the Cy and Ph moieties.

As stated earlier, high loading of POSS-grafted triblock copolymers have a perforated layer morphology. This morphology results in further decrease in *d* spacing in additional to the compatibility argument alone. The extent of perforation is also likely affected by the chemical substituents of POSS used.

Effect on the Order−Disorder Transition. The order−disorder transition behavior as affected by the presence of POSS attachments was examined using rheology and SAXS. In Figure 9, we compare the behavior of a pure SBS when it undergoes a transition from an order-state to a disorder-state as observed using rheology and SAXS. The left axis shows the storage modulus, $G'(\omega)$, as determined from rheology, and the right axis shows the peak width, Γ, as determined from SAXS; both are plotted over the same temperature range. In rheological experiments under a steady-state heat ramp, block copolymers exhibit a discontinuity in the plot of $G'(\omega)$ vs temperature. Here, the onset temperature of this discontinuity in $G'(\omega)$ is interpreted as T_{ODT}. In practice, T_{ODT} is a function of both frequency and temperature ramp rate, so the listed value does not coincide precisely with the "equilibrium T_{ODT}". However, this interpretation is consistently applied throughout the pure and POSS-grafted series, and thus, the effects of POSS attachments on the value of T_{ODT} are all comparable. The onset point was calculated by determining the intersection of a line fitted in the ordered morphological state below the T_{ODT} and a line fitted through the drop just after the T_{ODT}. The range of temperatures used for the fitting varied slightly based on the linearity of the two regions. The point of intersection for the two lines is largely influenced by the difference in slope of the fitted lines. Shallow or broad drops produce more uncertainty in the T_{ODT} determination. Sample-to-sample variation also contributes to T_{ODT} error and stems from morphological differences between prepared samples. Evaporation rates during the solvent-casting process must be similar, and annealing times must be long and of comparative duration to ensure reproducibility in copolymer morphology. If the solvent is evaporated too quickly or if the solvent is not completely removed during annealing, there will be noticeable changes in T_{ODT}. By performing multiple runs, sample variability was fractions of a degree for the casting/annealing scheme in place. Time sweeps were also performed at temperatures near T_{ODT} for some samples to ensure that confounding effects due to kinetics did not play a significant role in T_{ODT} determination.

SAXS was also used to determine the T_{ODT}. In SAXS experiments, there are two common ways to measure T_{ODT}: the discontinuity in the plot of 1/intensity vs $1/T$ or the discontinuity in the plot of $1/\Gamma$ vs $1/T$.[1,10,18,20] For the purposes of this paper, a plot of $1/\Gamma$ vs $1/T$ was used to determine the T_{ODT} from SAXS because the discontinuity was more distinct than that of the 1/intensity. The T_{ODT} was interpreted as the midpoint of the $1/\Gamma$ discontinuity.

A comparison of measured T_{ODT} data for SBS grafted with varying amounts of Ph-POSS is shown in Figure 10. Although both rheological and SAXS measurement showed the same trend of decreasing T_{ODT} with increasing POSS content, but there is

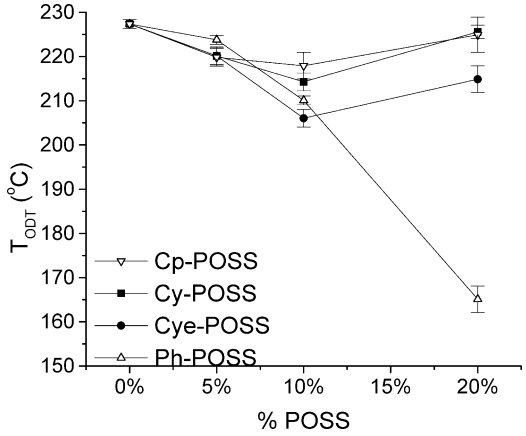

Figure 11. T_{ODT} of varying amounts of different moieties of POSS as determined using rheological measurement: (▽) cyclopentyl, Cp, POSS; (■) cyclohexenyl, Cy, POSS; (●) cyclohexenyl, Cye, POSS; (△) phenyl, Ph, POSS.

a disagreement in magnitude. Another observation is that the rheological experiments showed less error because they had sharper transitions and were more repeatable across multiple tests than the SAXS.

Rheological determination of T_{ODT} for SBS grafted with different amounts of Cp, Cy, Cye, and Ph-POSS moieties are plotted in Figure 11. For all POSS loadings, there is a decrease in the T_{ODT} relative to pure SBS. At low weight fractions, the data are similar in trend. At 5 wt % grafting, there is a 4−7 °C drop in T_{ODT} for all moieties. Increasing to 10 wt % grafting results in a further drop in T_{ODT} for all moieties. At large weight fractions of grafted POSS, there is a change in T_{ODT} trend. The T_{ODT} for the Ph-POSS continues to decrease significantly, but there is a divergence from this monotonic behavior for the Cp, Cy, and Cye moieties. This is attributed to the perforated layer morphology observed at high POSS loading. In this POSS-grafted SBS system, the perforated layer morphology is more thermally stable than the lamellar. Other block copolymer systems have made similar observations where $T_{ODT,\ PL} > T_{ODT,\ L}$.[30]

The Ph-POSS does not show a T_{ODT} increase at 20 wt % like the other moieties. Unlike the other moieties, the Ph-POSS has a much stronger affinity toward the styrene block. This may lead to slightly different phase behavior than the other moieties. In other words, the decrease in χ-parameter overcomes the contribution attributed to the perforated layer morphology.

Effect on the Rheology. In the rheological discussion below, we compare only Cy, Cye, and Ph-POSS grafted SBS because they have the same number of carbon atoms in similar stereochemistry, which reduces confounding effects due to size and molecular weight. Figure 12 shows the rheological data for the pure and 10 wt % POSS grafts. For the temperature ranges examined, the Ph-POSS has nearly the same storage modulus as the pure SBS while the Cy and Cye moieties show a higher value for the temperature-dependent storage modulus. The observed increase in storage modulus at low frequencies suggests that the POSS acts as reinforcement for the PB in the system or there is a change in morphology. The reinforcement for the Cy and Cye moieties may also be retained through the T_{ODT}, explaining the diminished drop in modulus after the onset of order−disorder transition. The 10 wt % Ph-POSS does not show a modulus increase. This is because the Ph moiety has a high affinity toward styrene segments; it is in effect plasticizing the SBS copolymer.

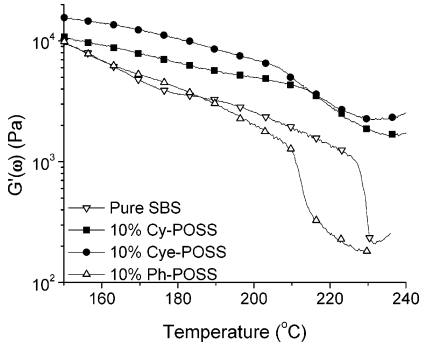

Figure 12. Storage modulus, $G'(\omega)$, as a function of temperature at 1 rad/s for pure and 10 wt % of POSS with specified moiety as indicated: (▽) SBS no POSS, POSS; (■) cyclohexenyl, Cy, POSS; (●) cyclohexenyl, Cye, POSS; (△) phenyl, Ph, POSS.

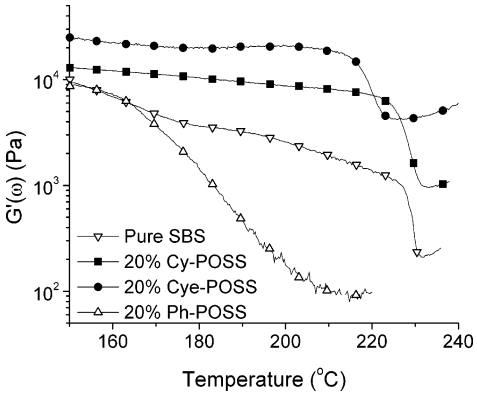

Figure 13. Storage modulus, $G'(\omega)$, as a function of temperature at 1 rad/s for pure and 20 wt % POSS with specified POSS moiety as indicated: (▽) SBS no POSS POSS; (■) cyclohexenyl, Cy, POSS; (●) cyclohexenyl, Cye, POSS; (△) phenyl, Ph, POSS.

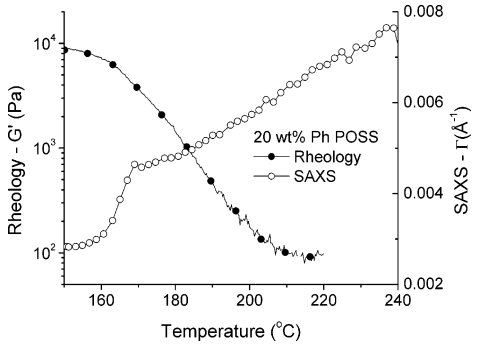

Figure 14. Rheological and SAXS T_{ODT} for 20 wt % Ph-POSS.

The rheological data for 20 wt % are shown in Figure 13. The T_{ODT} for the Cy and Cye moieties increases relative to the 10 wt % due to the morphology change. The observed increases in modulus may be due to a further POSS reinforcement in addition to the change in morphology. Other copolymers have noted an increase in the modulus on the order−order transition from a lamellar to a perforated layer morphology.[30]

The T_{ODT} of the 20 wt % Ph-POSS does not increase like that of Cp, Cy, and Cye moieties; however, the temperature range of the order−disorder transition as measured by rheology becomes broader. In Figure 14, we depict the rheological and SAXS data for 20 wt % Ph-POSS through the order−disorder transition on the same plot. Though the rheological transition is broad (spanning nearly 50 °C), the SAXS transition is narrower (about 10 °C). In each case, the respective transitions are broader than that of the pure SBS. This transition broadening, though magnified in this case, is observed in the other grafted

systems. This broadening of the order−disorder transition may be due to some changes in the kinetics as affected by the POSS attachment, the change to perforated layer morphology, or there may be a variance to the SBS phases caused by an increase in polydispersity/complex phase behavior.

IV. Conclusions

Using rheology and X-ray scattering, we have investigated the effect of grafting four sterically similar, yet electronically different, POSS derivatives onto the butadiene phase of SBS triblock copolymer with lamellar morphology. The addition of POSS to SBS alters the volume ratio of styrene and butadiene domains, and since the POSS is grafted to the butadiene block, it is chemically confined within the PB. However, the chemical substituents of POSS have a significant influence on the extent of segregation between butadiene and styrene phases. For the case of POSS with phenyl moiety, it has the highest affinity to the styrene phase, so when grafted to the butadiene it appears to be interacting well with the styrene phase. This causes not only the decrease in the lamellae *d* spacing but also a drop in the T_{ODT} due to an effect whereby the Ph-POSS plasticizes the SBS copolymer. The partly unsaturated Cye-POSS shows a somewhat lessened attraction to the PS phase, which in turn is greater than that exhibited by completely unsaturated Cy or Cp-POSS. For these moieties that have a lesser influence on the interaction between styrene and butadiene phases, the effect of POSS addition has a smaller impact on the change in *d* spacing and T_{ODT}. As the amount of POSS grafting increases, there is a change from a lamellar to a perforated layer morphology based on the results obtained from SAXS and rheology. This results in an anomalous shift in T_{ODT} for Cp, Cy, and Cye-POSS. The level of perforation and thermal stability of this morphology depends on the POSS moiety.

Acknowledgment. This research was partially supported by the Air Force Research Laboratory at Edwards AFB, CA. We are also thankful for the use of the synchrotron small-angle X-ray scattering facility at the Argonne National Laboratory. ChemMatCARS Sector 15 is principally supported by the National Science Foundation/Department of Energy under Grant CHE0087817 and by the Illinois Board of Higher Education. The Advanced Photon Source is supported by the U.S. Department of Energy, Basic Energy Sciences, Office of Science, under Contract W-31-109-Eng-38.

References and Notes

(1) Hamley, I. W. *The Physics of Block Copolymers*; Oxford University Press: New York, 1998.
(2) Binder, K. *Adv. Polym. Sci.* **1994**, *112*, 181.
(3) Leiber, L. *Macromolecules* **1980**, *13*, 1602.
(4) Fredrickson, G. H.; Helfand, E. *J. Chem. Phys.* **1987**, *87*, 697.
(5) Park, C.; Yoon, J.; Thomas, E. L. *Polymer* **2003**, *44*, 6725.
(6) Bates, F. S.; Fredrickson, G. H. *Annu. Rev. Phys. Chem.* **1990**, *41*, 525.
(7) Hanley, K. J.; Lodge, T. P. *J. Polym. Sci., Part B* **1998**, *36*, 3101.
(8) Lai, C.; Russel, W. B.; Register, R. A. *Macromolecules* **2002**, *35*, 841.
(9) Lodge, T. P.; Hanley, K. J.; Pudil, B.; Alahapperuma, V. *Macromolecules* **2003**, *36*, 816.
(10) Sakurai, S.; et al. *Macromolecules* **1992**, *25*, 2679.
(11) Adams, J. L.; Graessly, W. W.; Register, R. A. *Macromolecules* **1994**, *27*, 6026.
(12) Maurer, W. M.; et al. *J. Chem. Phys.* **1998**, *108*, 2989.
(13) Mai, S.; et al. *Macromolecules* **2000**, *33*, 5124.
(14) Hanley, K. J.; Lodge, T. P. *Macromolecules* **2000**, *33*, 5918.
(15) Tanaka, H.; Hasegawa, H.; Hashimoto, T. *Macromolecules* **1991**, *24*, 240.
(16) Lai, C.; Russel, W. B.; Register, R. A. *Macromolecules* **2002**, *35*, 4044.
(17) Banaszak, M.; Whitmore, M. D. *Macromolecules* **1992**, *25*, 3406.
(18) Floudas, G.; et al. *J. Chem. Phys.* **1997**, *106*, 3318.
(19) Lodge, T. P.; Pudil, B.; Hanley, K. J. *Macromolecules* **2002**, *35*, 4707.
(20) Xie, R.; Li, G.; Liu, C.; Jiang, B. *Macromolecules* **1996**, *29*, 5124.
(21) Biroš, J.; Zeman, L.; Patterson, D. *Macromolecules* **1971**, *4*, 30.
(22) Fu, B. X.; Lee, A.; Haddad, T. S. *Macromolecules* **2004**, *37*, 5211.
(23) (a) Lee, J. Y.; Park, M. S.; Yang, H. C.; Cho, K. W.; Kim, J. K. *Polymer* **2003**, *44*, 1705. (b) Krishnamoorti, R.; Giannelis, E. P. *Macromolecules* **1997**, *30*, 4102. (c) Ha, Y. H.; Thomas, E. L. *Macromolecules* **2002**, *35*, 4419.
(24) (a) Chun, S. B.; Mather, P. T. *Mater. Res. Soc. Symp. Proc.* **2001**, *661*, KK10.8/1. (b) Chun, S. B.; Kim, G. M.; Mather, P. T. "POSS-Grafted Block Copolymers for Nanostructured Surfaces", ACS National Meeting, Chicago, IL, Aug 2001.
(25) (a) Baney, R. H.; Itoh, M.; Sakakibara, A.; Suzuki, T. *Chem. Rev.* **1995**, *92*, 1409−1430. (b) Lichtenhan, J. D. *Comments Inorg. Chem.* **1995**, *17*, 115−130. (c) Lichtenhan, J. D. In *Polymeric Materials Encyclopedia*; Salamore, J. C., Ed.; CRC Press: New York, 1996; pp 7769−7778. (d) Li, G. Z.; Wang, L. C.; Ni, H. L.; Pittman, C. U. *J. Inorg. Organomet. Polym.* **2001**, *11* 123−154. (e) Phillips, S. H.; Haddad, T. S.; Tomczak, S. J. *Curr. Opin. Solid State Mater. Sci.* **2004**, *8*, 21−29. (f) Li, G. Z.; Pittman, C. U. In *Macromolecules Containing Metals and Metal-like Elements*; Abd El Aziz, A. S., Carraher, C. E., Pittman, C. U., Zeldin, M., Eds.; John Wiley & Sons: Hoboken, NJ, 2005; Vol. 5, Chapter 5, pp 79−131.
(26) Pangborn, A. B.; Giardello, M. A.; Grubbs, R. H.; Rosen, R. K.; Timmers, F. J. *Organometallics* **1996**, *15*, 1518.
(27) (a) Speier, J. L. Homogeneous catalysis of hydrosilation by transition metals. In *Advances in Organometallic Chemistry;* Academic Press: New York, 1979; Vol. 17, pp 407−447. (b) Marciniec, B.; Gulinski, J.; Urbaniak, W.; Kornetka, Z. W. In *Comprehensive Handbook on Hydrosilation*, Marciniec, Ed.; Pergamon: New York, 1992.
(28) Haddad, T. S.; Viers, B. D.; Phillips, S. H. *J. Inorg. Organomet. Polym.* **2001**, *11*, 155.
(29) NMR shift assignments for polybutadiene were taken from: Pham, Q. T.; Petiaud, R.; Walton, H.; Llauro-Darricades, M.-F. In *Proton and Carbon NMR Spectra of Polymers*; CRC Press: Ann Arbor, MI, 1991; p 117.
(30) (a) Matsen, M. W.; Thompson, R. B. *J. Chem. Phys.* **1999**, *111*, 7139. (b) Hajkuk, D. A.; et al. *Macromolecules* **1997**, *30*, 3788. (c) Förster, S.; et al. *Macromolecules* **1994**, *27*, 6922.

MA0518813